Part I
Self Assembly

Molecules at Work: Selfassembly, Nanomaterials, Molecular Machinery, First Edition. Edited by Bruno Pignataro.

1
Yoctoliter-Sized Vessels as Potential Biological Models

Sheshanath V. Bhosale, Bradley E. Wilman, and Steven J. Langford

Molecular assemblies are ubiquitous in nature as they are involved in the reversible formation of a wide variety of complex biological structures. An understanding of such molecular assemblies and the associated noncovalent interactions that connect complementary interacting molecular entities to surfaces is of central concern to structural biochemistry. Self-assembly on solid or colloidal surfaces is also emerging as a new strategy in chemical synthesis, with the potential of generating wholly synthetic structures for form or function with dimensions of $1–10^2$ nm [1].

Synthetically, nanostructures are manufactured by three different methods:

1) Controlled formation of covalent bonds
2) Through polymers
3) By molecular self-assembly.

Methods 1 and 2 have the distinct advantage of providing more accurate structures and analytics of the resulting nanostructures as they are less dynamic; however, they are often linked with a substantial experimental expenditure. The construction of discrete, well-defined nanostructures using molecular self-assembly has demonstrated how we, as scientists, have attained an astonishing degree of control over the noncovalent bond and associated thermodynamics. Two approaches are likely for further development of this field: solution-based and surface-derived functional systems utilizing molecular self-assembly [2]. This chapter investigates the development of the so-called yoctowells as a surface-functionalized material for studying molecular interactions.

1.1
Introduction

Among the biological processes known, photosynthesis is one of the most important. Photoactive molecules, brought together within a protein matrix with precise distance and orientation to facilitate an electron transfer process over

Molecules at Work: Selfassembly, Nanomaterials, Molecular Machinery, First Edition. Edited by Bruno Pignataro.

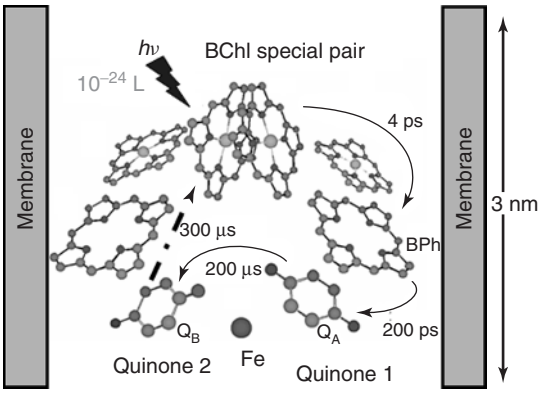

Figure 1.1 Model of a bacterial photosynthetic reaction center (PRC) for light-induced charge separation.

3 nm, are the key to the initial stages of photosynthetic reactions and hence life (Figure 1.1). By consuming carbon dioxide and liberating oxygen, photosynthesis has transformed the world into a hospitable environment. For decades, scientists have been fascinated by the photosynthetic reaction center (PRC) and its ability to transduce solar energy into electrical energy. There have been many approaches to identifying the factors that govern electron transfer, from small molecule dyads to large multichromophoric systems. One such approach, as highlighted recently by Matile and coworkers [3], makes use of core-substituted naphthalene diimides along a rigid-rod scaffold to generate a proton gradient across a lipid membrane. An earlier work by Moore and Gust [4] had introduced such a phenomenon by the application of a porphyrin–cartonoid–quinone conjugated system across a bilayer.

Chemists have been successful in the synthesis, isolation, and analysis of molecular machinery, but the mimicry of processes performed by natural systems, which have been developed over long-term evolutionary processes, still requires much attention. To gain understanding in this field, three general strategies have been employed in the past two decades for the preparation, entrapment, and ordering of molecules on a variety of surfaces: (i) lithographic [5], (ii) embossing [6, 7], and (iii) chemical-deposition methods [8, 9], that is, self-assembled monolayers (Figure 1.2).

Lithographic techniques have been employed to prepare many elegant examples such as hydrophilic pores of zeolite L crystals that have a diameter of 7.5 Å and are, as a result, able to include thousands of hydrated molecules such as electron-conducting methyl viologen or energy-transporting oligophenyl derivatives, which are thin enough to enter the gaps. Lithography is a destructive rather than constructive technique that still has problems at low-nanometer-level spatial resolutions, and as such problems can exist in establishing the precise intermolecular distances and number of molecules in each individual gap. Laser-assisted embossing on amorphous silicon can be used to form nanoscaled wells on the

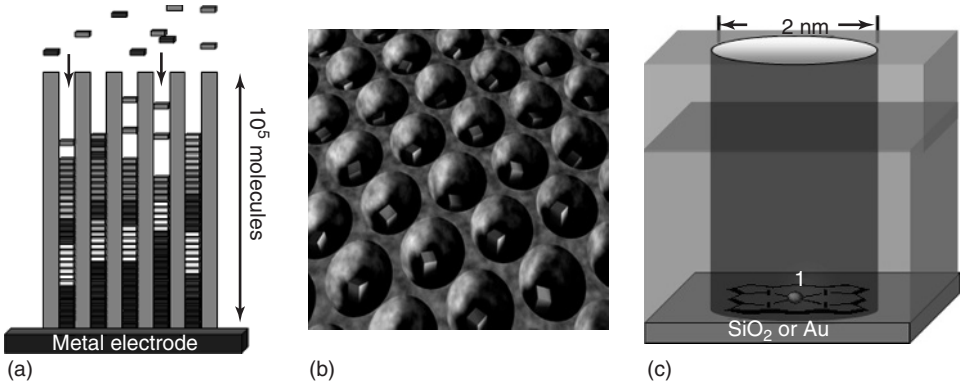

Figure 1.2 Model of the three general strategies (a) ordering of dye molecules in zeolite L channels, constructed by a lithographic method, (b) laser-assisted embossing producing zeptoliter cavities, which are used for growth of semiconductor molecules, and (c) self-assembled yoctowells are constructed by chemical deposition by applying two-step template strategy.

zeptoliter scale (1 zl = 10^{-21} l); these wells can be prepared in diameters as small as 50 nm. They can also be used as reaction vessels for the preparation of simple growth of inorganic salts and semiconducting nanocrystals with controlled sizes. Finally, the self-assembled containers formed by a template-directed strategy are the focus of this chapter.

1.2
Cavities on Glass Plates and Gold Surfaces

The chemical-deposition method has been demonstrated through the early work of the Sagiv group, in which molecules were covalently attached as Langmuir-Blodgett film (LB) monolayers on glass plates as carriers [10, 11]. Typically, trichlorooctadecylsilane is attached to the glass surface followed by the introduction of cyanine dyes with long alkyl chain substituents. However, problems experienced with the orientation of the dye molecules and with respect to the glass surface not being uniform limited this research from further development.

The preparation of gaps in monolayers was explored a decade ago by the group of Fuhrhop [12]. Typically, the monolayer of mercaptodiamido bolas was templated around a steroid or porphyrin moiety tightly bound parallel to the gold(I) surface, leading to gaps in the monolayers. Formation of the gaps was characterized by cyclic voltammogram techniques [13, 14]. This work demonstrated that 1,2-*trans*-cyclohexanediols and glucose can be actively sequestered from bulk water. Furthermore, there was a strong discrimination between 1,2-*cis*- and 1,2-*trans*-cyclohexanediols within the gaps. Later developments used citrate gold particles, which led to better reproducibility [15, 16]. Later research transferred

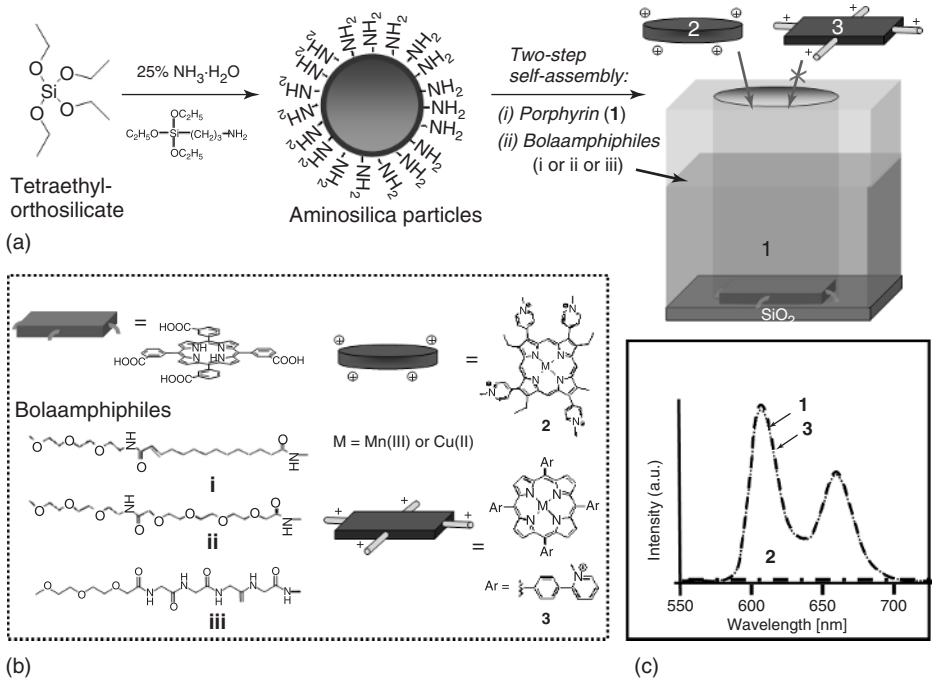

Figure 1.3 (a) Schematic showing yoctowell preparation on amino-functionalized silica particles, (b) structures used for preparation and size-exclusion study, and (c) discrimination study to confirm rigidity of the wells using fluorescence quenching.

this technology to colloidal silica as a means of offering more information through fluorescence measurements [17].

1.3 Preparation and Confirmation of Rigid Yoctowell Cavity

The silicate particles developed by van Blaaderen and Vrij [18] were produced in 1–10 g scales by hydrolysis of tetraethoxysilane with aqueous ammonia in ethanol in the presence of 3-aminopropyltriethoxysilicate (Figure 1.3a). Colloidal silica nanoparticles with a mean diameter of 100 nm were suitable for the self-assembly process. ''Yoctowells'' were constructed by a two-step procedure involving covalent attachment of an activated *meso*-(*tetra*-*m*-benzoic acid) porphyrin **1** with ethyl chloroformate followed by the reaction of diamido bolaamphiphiles (depending on choice) around **1**, leading to small wells of yoctoliter (10^{-24} l) size (Figure 1.3b) [17]. The wells had a diameter similar in width to **1** and height corresponding to the bola length. A total of 1500 yoctowells per particle or 20% surface coverage was a typical value.

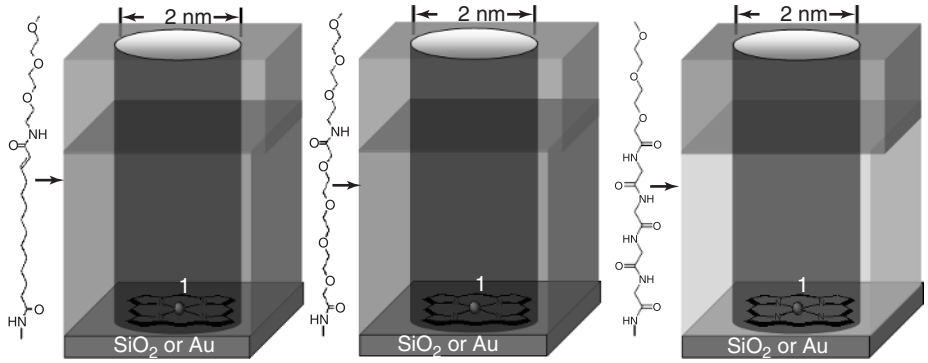

Figure 1.4 Models of the yoctowells hydrophobic (right), hydrophilic made up with rigid OEG walls (middle), and peptidic walls made up of triglycinyl bola (left).

1.3.1
Confirmation of Rigid Gaps

The gaps formed were confirmed by a discriminative fluorescence quenching assay in which the level of quenching of **1** was monitored as a function of the size of the quenching agent. For example, in the presence of **2**, which is of the same dimension as **1** (diameter ~2.2 nm), strong fluorescence quenching was observed. In the case of **3** (diameter ~3.6 nm), little fluorescence change was observed, inferring that size exclusion is possible as a result (Figure 1.3c). This also inferred that the integrity of the yoctowell was maintained throughout the experiment. Later, this was found to be a result of intermolecular hydrogen bonding between the bola.

The chemical versatility offered by the fabrication technique means that the walls of the yoctowells can be made using different phobicity as well as designed to include biological models (Figure 1.4). For example, bolas containing an alkyl chain produce hydrophobic wells, oligoethylene (OEG) chains produce hydrophilic wells, and triglycide bolas produce a peptidic internal environment [17, 19, 20].

1.4
Molecular Sorting

The rigidity and integrity of the yoctowell described through size-exclusion studies led to the formation of a molecular sorting protocol, where taking advantage of the slow and irreversible adsorption process of the included molecule could lead to the addition of a separate molecule (or more) through noncovalent and/or electrostatic forces [17]. The power of the sorting process was demonstrated through the preparation of porphyrin stacks in the order **A**, **B**, and **C** and **A**, **C**, and **B** within the yoctowells (Figure 1.5) [19].

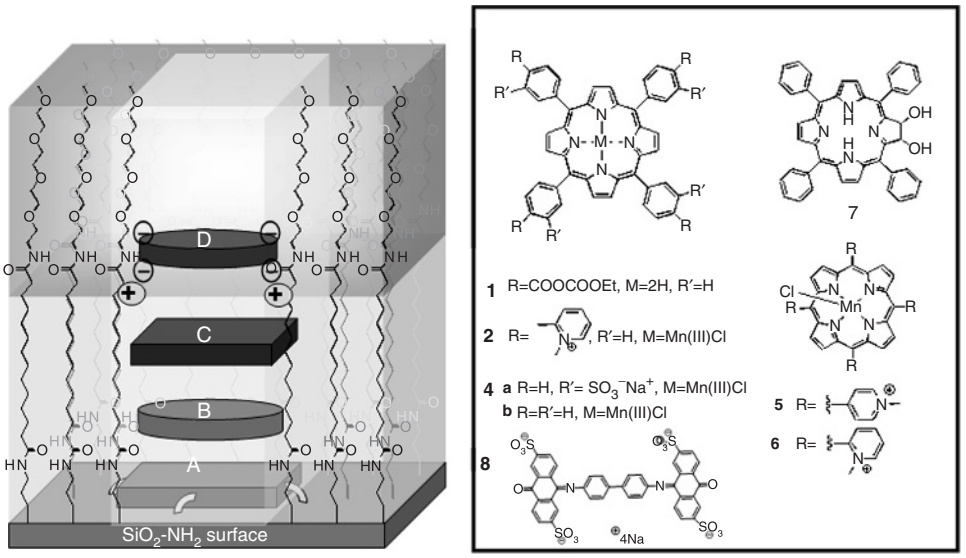

Figure 1.5 Model of the sorted molecules **A**, **B**, **C**, and **D** within yoctowell.

Taking this further, a heterotrimeric system comprising C_{60} was also prepared by taking advantage of π-electronic donor–acceptor interactions. The capping of the pores with anionic porphyrin showed the preclusion of C_{60}, demonstrating the importance of the sequential addition (Figure 1.6) [21]. The hydrophobic bolaamphiphile that forms the walls of these specific wells are made up of four important regions. The hydrophobic region stabilizes the fullerene within the pore via dispersion interactions and $\pi-\pi$ interactions between the fullerene and the bottom porphyrin **1**. Approximately 10 Å above the bottom porphyrin **1**, a ring of methylammonium groups is used for capping the pore with the tetrasulfonate **4** using electrostatic interactions. The third region bearing polyether groups solubilizes the outer sphere of the silica particle in aqueous solution.

The importance of the chemistry associated with the introduction of methylammonium groups around the periphery of the yoctowell is demonstrated in this next example. A judicial choice of the position of the ammonium groups by limiting the length of the bola and inclusion of an anionic acceptor leads to a series of molecular dyads for studying photo-induced charge separation [17]. The anionic quinone **8** and the Mn(III) anionic porphyrin **4**, which were added to the bulk water solution, were bound at the rim of the gap (Figure 1.7). Quenching of the bottom porphyrin fluorescence was observed depending on the distance; addition of a large excess of smaller quinone had no effect, indicating efficient capping [17, 22]. On excitation of the base porphyrin **1**, transient emission spectroscopy gives faster decay times of 0.028, 0.035, and 0.042 ns with varying amplitudes of 70–60%, when the anionic quinone is fixated at a distance of 5, 10, and 15 Å, respectively [22].

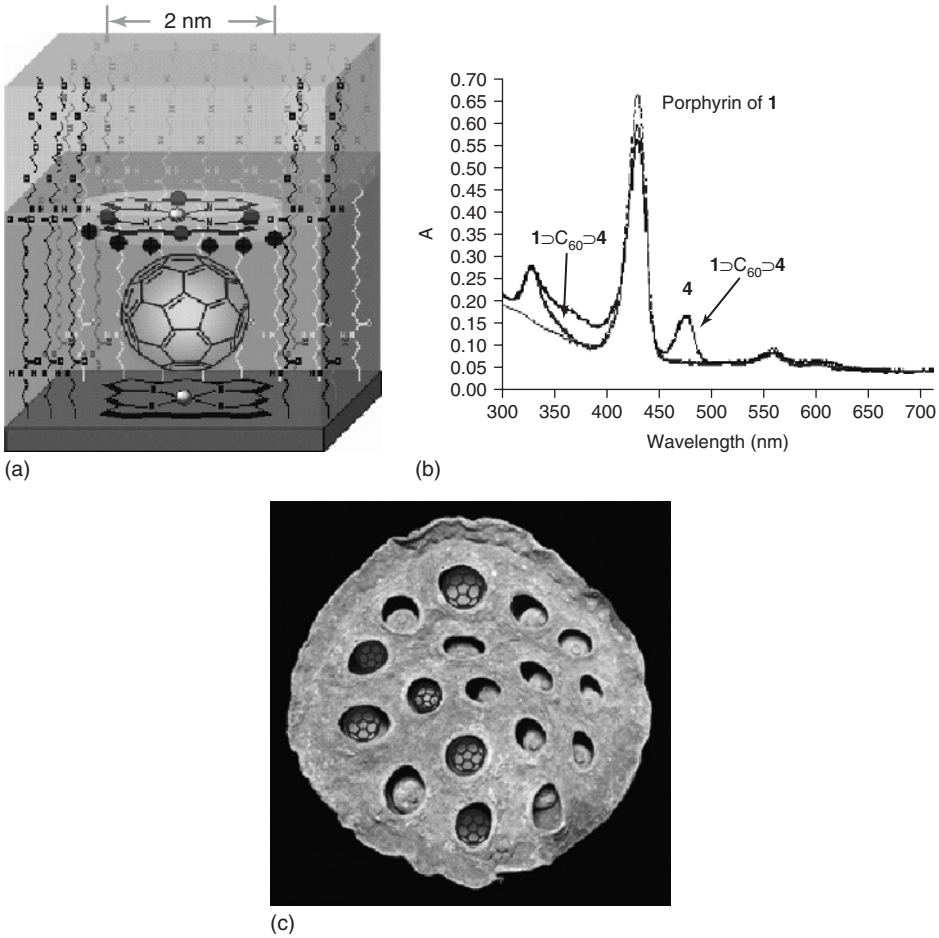

Figure 1.6 (a) Model of a yoctowell containing a trimeric (porphyrin–fullerene–porphyrin) stack, (b) UV–vis absorption spectroscopy trimeric dyes (**1** ⊃ C_{60} ⊃ **4**) within the pores of nanoscale dimensions, and (c) lotus fruit depicts this phenomenon well.

1.5 Yoctowell-Based Molecular Recognition Events

Considerable work had shown that yoctowells could be used to immobilize a series of different substrates including phenols (tyrosine, *o*-hydroquinone), carbohydrates (glucose, cellobiose, ascorbic acid), benzene, cyclohexane (1,2-*trans*-diol, 1,2-*trans*-diamine, 1,2-*trans*-dicarboxylate) and that these samples do not equilibrate with bulk water volumes over long periods as a result of ''immobilized hydration water,'' which stick to the walls of the hydrophobic yoctowells and cause a nanocrystallization event within the yoctowell [23]. To understand this inclusion

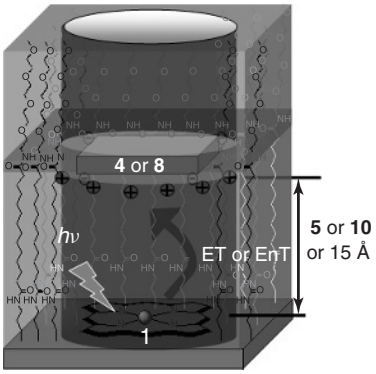

Figure 1.7 Model of two different dyes of different oxidation potentials.

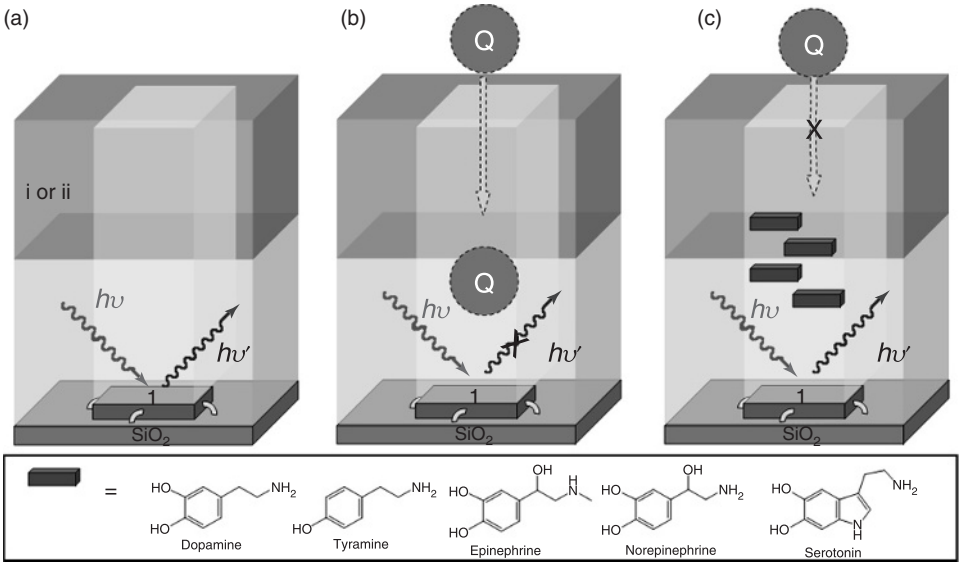

Figure 1.8 Excitation of bottom porphyrin **1** leads to fluorescence output (a), insertion of a quencher (Q) into the yoctowell causes fluorescence quenching (b), blocking of the yoctowell by a neurotransmitter that does not interfere with the fluorescence output of **1** and inhibits quenching by Q indicates an efficiency of binding (c).

phenomenon further, yoctowells comprising hydrophobic and hydrophilic walls have been used to investigate the discrimination of neurotransmitters [24], namely, dopamine, adrenaline, noradrenaline, tyramine, and serotonin in aqueous solution [25]. Findings have revealed that the hydrophobic yoctowells efficiently included most neurotransmitters; however, serotonin, which has a different overall structure, had little binding (Figure 1.8). In contrast, hydrophilic wells were shown to be more discriminant and weaker binders.

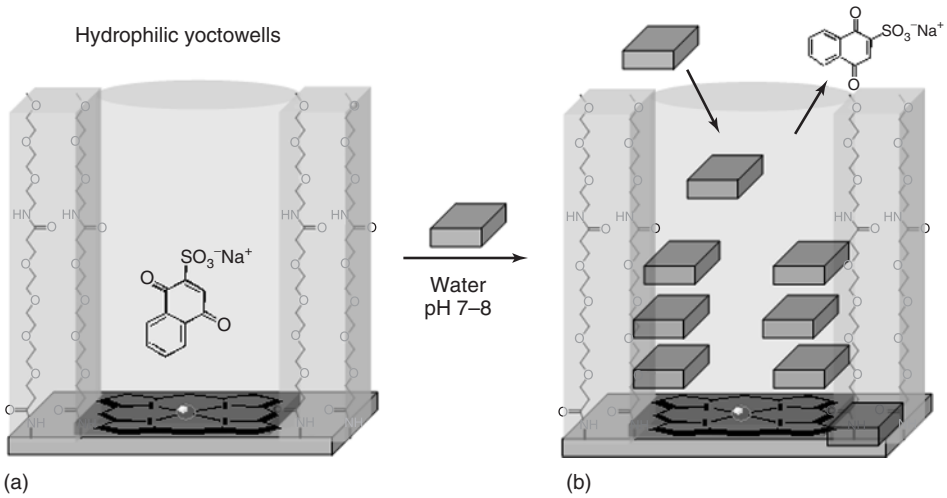

Figure 1.9 Yoctowells made up of oligoethylene bola and including a quinone that quenches bottom porphyrin fluorescence (a), entrapment of oligoamines (spermine, polylysine, and tobramycin) replaces quinone and binds tightly inside the cavity leading to fluorescence (b).

Hydrophobic yoctowells act as a size- and stereoselective kinetic trap for a range of solutes in water and offer exceptional means to study water-soluble molecules in these systems [23]. To check the hypothesis of ''hydrophobic kinetic trapping'' and also to apply the yoctowells for single polar molecules, yoctowells with tetraethyleneglycol walls were constructed. The new yoctowells bearing tetraethyleneglycol walls (Figure 1.9a) are similar to crown ethers, meaning oligoamines such as spermine, polylysine, and the rigid tricyclic tetraamine tobramycin are able to stick to the walls with binding constants on the order of $> 10^3\ M^{-1}$ at physiological pH (Figure 1.9). Titration of the filled oligoamine yoctowells with naphthoquinone 2-sulfonate failed to displace the guests. However, hydrophobic yoctowells containing only flexible OEG-head groups on the outer surface were shown not to bind oligoamines to any appreciable amount [20].

1.6 Conclusion

Yoctowell-recognition systems are likely to contribute to a new generation of bioinspired materials in *biotechnology* and *nanotechnology*, high-throughput identification screening systems, and provide a new approach toward energy-transduction systems [26]. Furthermore, the ability to form informative nanoscale assemblies will be vital to advances in the development of novel sensors and techniques for medical, biochemical, industrial, and environmental applications. One may apply these yoctowells to instances of sorting of two or more molecules leading to controlled release.

Acknowledgments

This work was supported by the Australian Research Council for support under the Discovery program (DP0878756). S.V.B. is grateful to the ARC for an APD fellowship.

References

1. Whitesides, G.M., Mathias, J.P., and Seto, C. (1991) *Science*, **254**, 1312–1319.
2. Lehn, J.-M. (1995) *Supramolecular Chemistry: Concepts and Perspectives*, Wiley-VCH Verlag GmpH.
3. Bhosale, S., Sission, A.L., Talukdar, P., Furstenberg, A., Banerji, N., Vauthey, E., Bollot, G., Mareda, J., Roger, C., Wurthner, F., Sakai, N., and Matile, S. (2006) *Science*, **313**, 84–86.
4. Gust, D., Moore, T.A., and Moore, A.L. (2001) *Acc. Chem. Res.*, **34**, 40–48.
5. Buyukserin, F., Kang, M., and Martin, C.R. (2007) *Small*, **3**, 106–110.
6. Barton, J.E. and Odom, T.W. (2004) *Nano Lett.*, **4**, 1525–1528.
7. Kang, M., Yu, S., Li, N., and Martin, C.R. (2004) *Langmuir*, **21**, 8429–8438.
8. Bhosale, S.V. and Langford, S.J. (2007) *Org. Biomol. Chem.*, **5**, 3733–3744.
9. Wang, T., Bhosale, S., Bhosale, S., Li, G., and Fuhrhop, J.-H. (2006) *Acc. Chem. Res.*, **39**, 498–508.
10. Polymeropoulos, E.E. and Sagiv, J. (1978) *J. Chem. Phys.*, **69**, 1836–1847.
11. Sagiv, J. (1980) *J. Am. Chem. Soc.*, **102**, 92–98.
12. Fuhrhop, J.-H., Bedurke, T., Gnade, M., Schneider, J., and Doblhofer, K. (1997) *Langmuir*, **13**, 455–459.
13. Fudickar, W., Zimmermann, J., Ruhlmann, L., Schneider, J., Roeder, B., Siggel, U., and Fuhrhop, J.-H. (1999) *J. Am. Chem. Soc.*, **121**, 9529–9545.
14. Skupin, M., Li, G., Fudickar, W., Zimmermann, J., Roder, B., and Fuhrhop, J.-H. (2001) *J. Am. Chem. Soc.*, **123**, 3454–3461.
15. Li, G. and Fuhrhop, J.-H. (2002) *Langmuir*, **18**, 7740–7747.
16. Li, G., Doblhofer, K., and Fuhrhop, J.-H. (2002) *Angew. Chem. Int. Ed.*, **41**, 2730–2734.
17. Li, G., Bhosale, S.V., Wang, T., Hackbarth, S., Roeder, B., Siggel, U., and Fuhrhop, J.-H. (2003) *J. Am. Chem. Soc.*, **125**, 10693–10702.
18. van Blaaderen,A. and Vrij, A.J. (1993) *Colloid Interfacial Sci.*, **156**, 1.
19. Bhosale, S.V., Bhosale, S., Wang, T., Li, G., Siggel, U., and Fuhrhop, J.-H. (2004) *J. Am. Chem. Soc.*, **125**, 13111–13118.
20. Bhosale, S., Bhosale, S., Wang, T, Kopaczynska, M., and Fuhrhop, J.-H. (2006) *J. Am. Chem. Soc.*, **128**, 2156–2157.
21. Bhosale, S.V., Bhosale, S.V., Langford, S.J., and Krsta, D. (2009) *Chem. Commun.*, 3166–3168.
22. Bhosale, S.V., Hackbarth, S., and Langford, S.J. (2011) *Chem. Asian J.*, doi: 10.1002/asia.201100533.
23. Bhosale, Sh., Li, G., Li, F., Wang, T., Ludwig, R., Emmler, T., Buntkowsky, G., and Fuhrhop, J.-H. (2005) *Chem. Commun.*, 2559–2561.
24. Mosharov, E.V., Gong, L.-W., Khanna, B., Sulzer, D., and Lindau, M.J. (2003) *Neuroscience*, **23**, 2835–2844.
25. Bhosale, S.V., Langford, S.J., and Bhosale, S.V. (2009) *Supramol. Chem.*, **21**, 18–23.
26. Bhosale, S.V., and Langford, S.J. (2011) *Chem. Soc. Rev.*, DOI: 10.1039/C1CS15152E.